Impurity doping in SiO_2: Formation energies and defect levels from first-principles calculations

Dong Han,[1] D. West,[2] Xian-Bin Li,[1] Sheng-Yi Xie,[1] Hong-Bo Sun,[1,3] and S. B. Zhang[1,2]
[1]*State Key Laboratory on Integrated Optoelectronics, College of Electronic Science and Engineering, Jilin University, 2699 Qianjin Street, Changchun 130012, China*
[2]*Department of Physics, Applied Physics, and Astronomy, Rensselaer Polytechnic Institute, Troy, New York 12180, USA*
[3]*College of Physics, Jilin University, 119 Jiefang Road, Changchun 130023, China*
(Received 7 June 2010; revised manuscript received 22 September 2010; published 22 October 2010)

Substitutional doping properties of silicon dioxide are investigated systematically with *ab initio* calculations. The dopants include a range of elements from group-III, group-V, and group-VII. We find that SiO_2 has a relatively symmetric doping profile in terms of its ionization energies, i.e., relatively shallow acceptor levels and donor levels are both predicted, despite its wide experimental band gap of 9.65 eV. The best candidates for *p*-type and *n*-type doping are Al_{Si} and P_{Si} with calculated ionization energy of 0.86 eV and 0.74 eV, respectively, both being less than 10% of the total band gap. Larger doping asymmetry exists in terms of the impurity formation energy: under optimum (O-rich) growth conditions, the shallowest acceptor, Al_{Si}, and donor, P_{Si}, have formation energies of 1.75 eV and 3.05 eV, respectively. These results provide theoretical insights on how to make this previously considered absolute insulator work as a wide-gap semiconductor at elevated temperatures.

DOI: 10.1103/PhysRevB.82.155132 PACS number(s): 61.72.J−, 71.55.−i

I. INTRODUCTION

Silicon dioxide (SiO_2), an abundant resource in nature, holds an important status in various applications due to its excellent optical and electrical properties.[1] For instance, glass fiber is regarded as the basis of modern communication.[2,3] In the metal-oxide-semiconductor (MOS) based microelectronic industry, SiO_2 has been widely used as the isolated gate. However, the performance of SiO_2 is influenced by the presence of various impurities. A large number of experimental and theoretical studies have been devoted to evaluate the impurity effect on its optical or electrical properties.[4–17] For example, cationic impurities, such as aluminum or boron have been studied by optical absorption spectra.[13,18] While it is generally accepted that these impurities would produce a series of distinct electronic levels in the band gap, other dopants have been found to significantly enhance the photosensitivity of SiO_2. Phosphorus is a case. With phosphorus doping the efficiency of rare-earth based optical fiber amplifier is greatly increased. Furthermore, phosphosilicate glass is considered to be a good candidate for radiation sensors due to its near linear response to radiation dose.[9,19,20] Yet other impurities have been studied with regard to improvement of the dielectric characteristics in the usage of the MOS devices, for instance, nitrogen substituting oxygen as a Si-O-N alloy can substantially enhance its dielectric constant.[14,21]

Until now many efforts on SiO_2 doping focus on improving the application-demand characteristics. Due to the very large band gap of SiO_2 (9.7 eV), it is generally accepted that SiO_2 is exclusively an insulator. However, diamond was also commonly believed to be an insulator due to its relatively large band gap of 5.5 eV before the achievement of *p*-type doping.[22] As a matter of fact, the boundary between semiconductors and insulators is becoming more and more difficult to define, in light of recent success in doping wide-gap materials such as AlN and ZnMgO for future ultraviolet optoelectronic devices.[23,24] This raises an interesting and important question: can SiO_2 also be doped to become a semiconductor? Since SiO_2 is known to be the largest-gap inorganic solid, it is an excellent test case for doping wide-gap insulators.

In this paper, we address this question through systematic calculations of the doping properties of substitutional impurities in SiO_2. The acceptors include group-III elements (B_{Si}, Al_{Si}, and Ga_{Si}) and group-V elements (N_O, P_O, and As_O), whereas the donors include group-V elements (N_{Si}, P_{Si}, and As_{Si}) and group-VII elements (F_O, Cl_O, and Br_O). We find that, in general, the group-III-on-group-IV impurities have shallower acceptor levels and the group-VII-on-group-VI impurities have shallower donor levels. These can be understood because a group-III-on-group-IV site would not directly perturb the valence-band maximum (VBM) which is oxygen derived. Similarly, a group-VII-on-group-VI site would not directly perturb the conduction-band minimum (CBM) which is silicon derived. However, there is an important exception; namely, P-on-Si has by far the shallowest donor level, being 0.74 eV below the CBM. In contrast, the shallowest acceptor level, Al-on-Si, is 0.86 eV above the VBM. The corresponding impurity formation energies, at the most favorable oxygen rich growth condition, are 3.0 eV and 1.7 eV, respectively. We can estimate the solid solubilities at the SiO_2 melt temperature of 1650 °C to obtain 10^{15} cm^{-3} and 10^{18} cm^{-3} for phosphor and aluminum doping, respectively. With today's doping techniques, one may boost the doping level considerably from the solid solubility level by nonequilibrium doping. These results thus suggest that doping SiO_2 for electronic and optoelectronic applications may be possible at least at elevated temperatures.

II. CALCULATION METHODS

We perform first-principles calculations based on the density-functional theory (DFT),[25,26] as implemented in the

VASP codes.[27] Projector augmented wave basis[28] and generalized gradient approximation (GGA)[29] with the Perdew-Burke-Ernzerhof functional[30] are employed. The structure used is α quartz, which is the most stable crystalline allotrope of SiO_2 at STP. A 72-atom based $2\times2\times2$ supercell is used throughout the calculations. All of the atoms are allowed to relax until Hellman-Feynman force is less than 0.03 eV/Å. The cutoff energy and Monkhorst-Pack k-point mesh grid are 540 eV and $2\times2\times2$, respectively. Note that DFT possesses residual self-interaction for electrons. As such, it cannot accurately describe the local configuration for defects in strong electron-localized systems.[31] SiO_2 falls into this category due to its strong ionic character. It has been shown that the GGA+U method can reduce the error due to self-interaction to yield defect structures consistent with experiment.[32] Here, we use GGA+U for both geometry relaxation and the evaluation of defect formation energy. After several tests, a U with 7 eV is endowed to the O $2p$ orbital.[33] It is well known that GGA underestimates the band gap. In the present case, the calculated band gap for SiO_2 with GGA and GGA+U is 5.88 eV and 6.54 eV, respectively.

To determine the electrical effects of impurities, we focus on the formation energies of impurity-related defects as well as their transition levels. The formation energy of a dopant determines the possibility of its existence in SiO_2. The formation energy, $E^f(X_Y^q)$, of element X substituting for element Y in a bulk crystal is obtained from[34] as follows:

$$E^f(X_Y^q) = \Delta E(X_Y^q) - \mu(X) + \mu(Y) + qE_F, \tag{1}$$

where, X is the impurity atom and Y is the replaced host atom.

$$\Delta E(X_Y^q) = E_{tot}(X_Y^q) - E_{tot}(bulk) - \mu(X)_{solid/gas} + \mu(Y)_{solid/gas} + q\varepsilon_{\mathrm{VBM}}. \tag{2}$$

Here, $E_{tot}(X_Y^q)$ is the total energy of a supercell containing the substitutional dopant X (replacing Y) with charge q and $E_{tot}(bulk)$ is the total energy of the same bulk supercell. $\mu(X)_{solid/gas}$ and $\mu(Y)_{solid/gas}$ are the chemical potentials of elements X and Y at solid/gas form. $\varepsilon_{\mathrm{VBM}}$ is the VBM of the host supercell. $\mu(X)$ and $\mu(Y)$ are the chemical potential of the elements X and Y referenced to $\mu(X)_{solid/gas}$ and $\mu(Y)_{solid/gas}$. Since the formation of dopants relate to the experimental growth or annealing environment, e.g., Si-rich condition, O-rich condition, or between them, the formation energy must depend on the chemical potential of X, Y, reflected by the environment. Under thermal equilibrium, the chemical potential of host atoms must satisfy $\mu(\mathrm{Si})+\mu(\mathrm{O}) = \Delta H(SiO_2)$, where $\Delta H(SiO_2)$ is the formation enthalpy of SiO_2 with the form of α quartz. Depending on the experimental condition, $\mu(\mathrm{Si})$, $\mu(\mathrm{O})$ can vary in the range,

$$\text{(Si-poor condition)}\Delta H(SiO_2) \le \mu(\mathrm{Si}) \le 0 \text{ (Si-rich condition)}, \tag{3}$$

$$\text{(O-poor condition)}\frac{\Delta H(SiO_2)}{2} \le \mu(\mathrm{O}) \le 0 \text{ (O-rich condition)}. \tag{4}$$

From the calculated formation energies, which for charged defects explicitly depend on E_F, we determine the thermodynamic transition levels of the defects. The transition level, defined as the value of E_F where the different charge states have the same formation energy, can be written as follows:

$$\varepsilon(q/q') = \frac{[\Delta E(X_Y^q) - \Delta E(X_Y^{q'})]}{q' - q}, \tag{5}$$

where q and q' are the two different charge states of the substitutional dopant, e.g., an acceptor transition level, $\varepsilon(0/-1)$, is the Fermi energy at which the acceptor defect has equal energy in the two different charge states, $q=0$ and $q'=-1$, whereas a donor transition level, $\varepsilon(+1/0)$, is the Fermi energy at which the donor defect has equal energy in the two different charge states, $q=1$ and $q'=0$.

While Eq. (5) yields the transition energy within the calculated band gap of 6.54 eV, there exists a substantial deviation from the experimental gap of 9.65 eV.[35] This large discrepancy, of over 3 eV, is of particular concern in the determination of whether a defect is shallow or deep, so care must be taken in order to determine how the defect levels shift as the gap is opened. In this work, we make an effort to overcome this problem with the wave-function-projection method (WPM).[36] That is that when we raise the conduction band to meet the experimental gap the transition levels are modified according to the projected ratio of the defect state on the VBM and CBM at the Γ point of the Brillouin zone. This method has been shown to give reasonable results.[37]

III. RESULTS AND DISCUSSIONS

A. Atomic geometry

In α quartz, each Si atom and its four neighboring O atoms form a SiO_4 tetrahedron with C_2 symmetry. For most impurities, the tetrahedron for the neutral substitutional impurity X_{Si}^0 (X refers to every dopant) is preserved in LDA calculations.[10] In contrast, our GGA+U calculations destroy the C_2 symmetry of the tetrahedron. Most of our calculations are consistent with electron paramagnetic resonance (EPR) or electron spin resonance experiment, including both local structure and spin electron distribution.[4–6,38,39] The only exception being N_{Si}^0, where it is difficult to find an experiment result of an NO_4 tetrahedron in quartz. That, however, can be attributed to its high formation energy, which will be discussed later. Figures 1(a) and 1(b) show the relaxed local configuration of Si-substituted impurities and their corresponding bond lengths. For group-III acceptors, one of the X-O bonds elongates significantly. Compared to the remaining three, the elongated bond is increased by 44.7%, 10.6%, and 12.7% for B, Al, and Ga, respectively. For group-V donors, N has the similar bond-length variation that one bond ($\mathrm{N\text{-}O}^2$) is 54.4% longer than the other three, whereas P and As maintain the C_2 symmetry. For P and As, two pairs of bonds are elongated (X-O^2 and X-O^3), leaving a shorter pair

a)

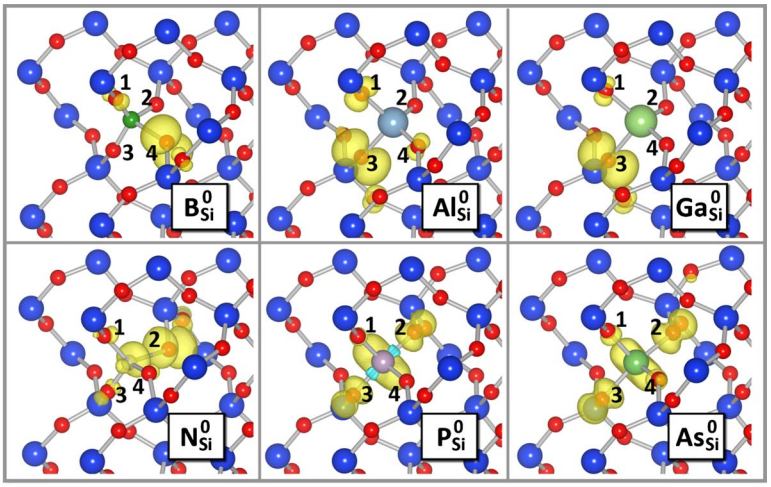

b)

Impurities	B	Al	Ga	N	P	As
O^1	1.378	1.701	1.809	1.404	1.590	1.766
O^2	1.377	1.687	1.792	**2.181**	**1.680**	**1.857**
O^3	1.382	**1.870**	**2.024**	1.427	**1.701**	**1.901**
O^4	**1.996**	1.685	1.787	1.408	1.586	1.760

Si
O

FIG. 1. (Color online) The calculated atomic geometry and the spin electron density for neutral X_{Si} defects is shown in (a). The isosurface of spin electron density is $0.005/a_0^{-3}$, where a_0 is the Bohr radius. The distance between neighbor oxygen and the impurity is listed in (b), the longest bond length and the second longest bond length (only for P and As) between impurities and neighboring O atoms are darkened. The four neighboring O atoms are labeled in the atomic geometry.

of bonds (X-O^1 and X-O^4). The spin electron density distributions [see Fig. 1(a)] clearly reveal the origin of the local distortion, which could be classified as Jahn-Teller distortion.[40] For group-III dopants, their spin charge is mainly localized in the $2p$ orbital of the elongated-bond oxygen atom. Due to the C_2 symmetry of the SiO_4 tetrahedron in bulk (one pair of long bonds and one pair of short bonds) the $2p$ orbital of O is doubly degenerate. When a group-III dopant (three valence electrons) replaces Si (four valence electrons), the structure is stabilized when the hole occupies the local orbital, with the degeneracy removed, rather than the nonlocal degenerate orbital [see Fig. 1(a)]. This hole weakens the Coulomb binding between the dopant and one of the oxygen, elongating their distance. For the N impurity of group-V, the extra unpaired electron does not occupy the bonding states but antibonding state overlapped by one $O(O^2)2p$ orbital and N sp^3 hybrid orbital. Hence this antibonding state weakens the covalent bond of N-O^2, leading to a substantial extension of the N-O^2 bond. However, it is quite different for case of P and As which should be attributed to the existence of unoccupied d orbital. For the P dopant, the antibonding state, which is occupied by the unpaired electron, is made up of its $3d$ orbital and the $2p$ orbital of the related O (O^2 and O^3). This is why the spin charge dominates the region around the extended P-O^2 bond and P-O^3 bond. Moreover, the increased angle of O^2-P-O^3 shows more or less the characteristics of d orbital bonding. The local structure for As is similar to that for P, the only difference being that each of the As-O bonds are slightly longer than the corresponding P-O bonds. Chemically, the only difference is that the occupied antibonding state is made up of $4d$ orbital of As and $2p$ orbital of two related O (O^2 and O^3).

B. Formation energy

Growth conditions can greatly affect the formation energies of defects. In SiO_2, further considerations must be made due to the number of secondary compounds, which can limit the range of growth conditions. To avoid the formation of the secondary compound X_mZ_n (where Z is a host atom, O or Si), the chemical potential must also satisfy $m\mu(X)+n\mu(Z) \leq \Delta H(X_mZ_n)$, where $\Delta H(X_mZ_n)$ is the formation enthalpy of the secondary compound. From the equations above, the formation energy is greatly limited by the formation enthalpies of the secondary compounds. Table I shows the calculated formation enthalpies of SiO_2 and the possible secondary compounds. From the comparison with experiment, it can be seen that while the formation enthalpies for the nonoxides are quite reasonable, those of the oxides have a relatively large error. This error for the oxides is mainly due to the U parameter for energy calculation. However, as we detailed in Sec. II, the U parameter is critical for reproducing reasonable

TABLE I. Calculated and experimental formation enthalpies, ΔH_f, for SiO_2 and the possible secondary compounds. For the calculation of formation enthalpy, we add U parameters (U=7 eV) both on O $2p$ orbital of oxides and O_2 molecule which is consistent with our procedure for geometry relaxation.

Compound (phase)	ΔH_f (Calc.) (eV)	ΔH_f (Expt.)[a] (eV)
SiO_2 (s)	−7.72	−9.47
Al_2O_3 (s)	−13.90	−17.40
As_2O_5 (s)	−5.33	−9.25
B_2O_3 (s)	−10.94	−13.07
Ga_2O_3 (s)	−7.98	−11.29
P_2O_5 (s)	−11.55	
Si_3N_4 (s)	−7.73	−7.73
SiF_4 (g)	−15.63	−16.77
$SiCl_4$ (g)	−6.43	−6.82
$SiBr_4$ (g)	−4.64	−4.31

[a]Reference 41.

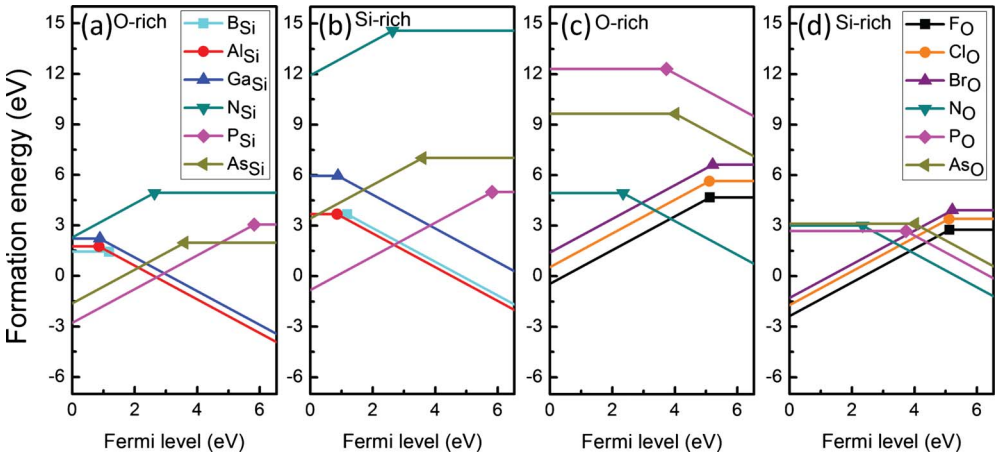

FIG. 2. (Color online) Calculated formation energies as a function of Fermi level for the substitutional defects. Si-substituted defects with neutral or ± 1 charged states are shown in (a) and (b). O-substituted defects with neutral or ± 1 charged states are shown in (c) and (d). Formation energies of defects are shown for [(a) and (c)] O-rich conditions and [(b) and (d)] Si-rich conditions. The Fermi level varies from 0 at VBM to 6.54 eV at CBM, which is the calculated band gap of SiO_2 with GGA+U. Figures 2(a) and 2(b) have the same legend panel shown in (a). Figures 2(c) and 2(d) have the same legend panel shown in (d).

localized geometries of the defect structures. While this leads to some unavoidable error in the domain of the allowable chemical potentials, which is reflected in the formation energies, it should be noted that this in no way affects the defect transition levels.

For charged defects, the formation energy is also a function of Fermi energy (E_F), as defined in Eq. (1). The E_F varies from the VBM to the CBM according to the band gap of α quartz. Here, we directly apply the calculated band gap with GGA+U to define the variation in E_F. The formation energies of the substitutional dopants, as a function of E_F, are shown in Fig. 2. For neutral impurities, we can clearly see that the Si-substituted dopants have lower formation energies at the O-rich condition [see Fig. 2(a)], whereas the O-substituted dopants have lower formation energies at Si-rich condition [see Fig. 2(d)]. In fact, it makes sense that at the O-rich condition the low concentration of O vacancy hinders the O-substituted doping but the high concentration of Si vacancy facilitates the Si-substituted doping and vice versa at Si-rich condition. From the calculated results shown in Fig. 2, the formation energies of the neutral group-III acceptors (B_{Si}, Al_{Si}, and Ga_{Si}) are fairly low under O-rich conditions, being 1.44 eV, 1.75 eV, and 2.23 eV, respectively. In contrast, acceptors are much more difficult to form at the Si-rich condition; the lowest formation energies for neutral acceptors being the group-V acceptors (N_O, P_O, and As_O) with formation energies of 3.01 eV, 2.68 eV, and 3.11 eV, respectively. For the case of donors, the lowest formation energy of the neutral group-V donors (N_{Si}, P_{Si}, and As_{Si}) are 4.92 eV, 3.05 eV, and 1.97 eV, respectively, at O-rich condition and the lowest ones for the neutral group-VII (F_O, Cl_O, and Br_O) donors are 2.75 eV, 3.39 eV, and 3.92 eV, respectively, at Si-rich condition. In fact, the formation energy for the dopants in SiO_2 exhibits a broad variation region. It can be traced back to the wide band gap of SiO_2 and the relatively large formation enthalpy of SiO_2. Based on the formation energy, acceptors (group-III at the Si site) should be quite easy to dope, with group-V at the O site being more difficult. The doping of donors is more problematic due to the generally higher formation energies. However, most donors formation energies are less than 3.4 eV except N_{Si} and Br_O. Adequate doping concentrations may thus be attained with modern nonequilibrium doping techniques.

C. Transition level

The transition levels of the substitutional dopants are shown in Fig. 3. A comparison of the results with and without the WPM correction shows that the impurity levels with respect to the respective band edges do not change due to the correction. For example, the acceptor levels relative to the VBM increase typically by less than 0.01 eV; the donor levels relative to the CBM decrease typically by less than 0.03 eV. The only exception is N_{Si} for which the decrease is 0.33 eV (more discussion on this exceptional and relatively large shift will be given below). The virtually null result of the projection is quite informative given the relative deepness of all the impurity levels (>0.9 eV). It suggests that for SiO_2 with a 9.65 eV band gap, a state 2–3 eV deep inside the band gap is predominantly a band edge state, most likely with physical properties similar to those of its parent states.

For acceptors, the transition levels of group-III dopants B_{Si}, Al_{Si}, and Ga_{Si} (1.18 eV, 0.86 eV, and 0.88 eV above the VBM, respectively) are substantially lower than that of group-V dopants N_O, P_O, and As_O (2.34 eV, 3.73 eV, and 4.02 eV above the VBM, respectively). This can be understood by noting that the VBM is mainly derived from the O 2p orbital. The Si-substituted acceptors induce a smaller perturbation than the O-substituted acceptors do. For B_{Si}, Al_{Si}, and Ga_{Si}, the small differences in the relative positions of their transition level can be attributed to the degree to which the hole is localized. This is reflected in the local geometry, for instance, the Al impurity can be regarded as the shallowest acceptor mostly due to the relatively small elongation of its X_{Si}-O bond compared to B and Ga. For the group-V impurity acceptors (O substituted), the transition

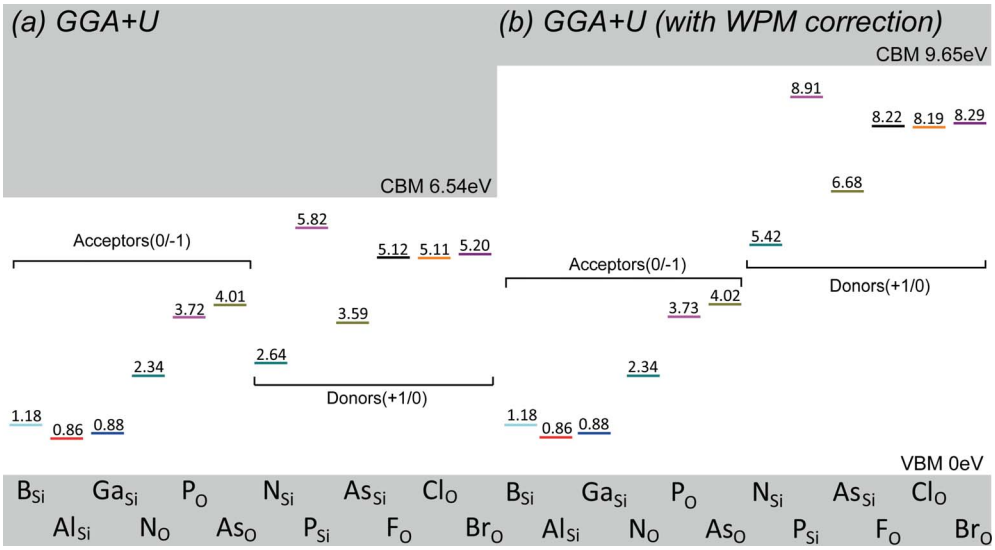

FIG. 3. (Color online) The calculated thermodynamic transition levels for substitutional defects before and after modification in SiO_2. The value of transition levels are shown with respect to VBM. (a) The position of the transition levels and the calculated band gap with GGA+U. (b) The transition levels after application of the wave-function-projection method and the experimental band gap.

level is more simply related to their electronegativity, it being easier to put an electron on a more electronegative atom. Hence, as the substitutional atom becomes less electronegative N, P, and then As, the corresponding defect level becomes deeper.

A similar result is found for the case of donors. The transition levels of the group-VII dopants (F_O, Cl_O, and Br_O), being 1.43 eV, 1.46 eV, and 1.36 eV below the CBM, respectively, are generally shallower than those of the group-V dopants (N_{Si}, P_{Si}, and As_{Si}), being 4.23 eV, 0.74 eV, and 2.97 eV below the CBM, respectively. The explanation for this behavior is similar to the acceptors but here it is the O-substituted donors which perform only a small perturbation on CBM, mainly yielding shallower donor levels than the Si substituted donors. The notable exception is P_{Si}, which has the shallowest level of all the donors investigated, at only 0.74 eV below the CBM. The position of the donor levels of group-V dopants at the Si site (much like as acceptors at the O site) are primarily determined by their atomic levels and subsequent relaxation. From their behavior in crystalline Si, one might expect both P and As to introduce shallow donor levels.[42] While this is true for the case of P_{Si} (which retains the crystal symmetry with very little relaxation), As_{Si} undergoes local structural distortion, as indicated in the geometry section, leading to a substantial deepening of the donor level of As_{Si}, and hence becoming markedly deeper than that of P_{Si}. N_{Si}, on the other hand, is quite deep; this is not only due to the large ionization energy of the N atom but also due to the broken N-O bond, as shown in Fig. 3(a).

In the light of the transition levels for the considered dopants, the best candidate for n-type doping and p-type doping are predicted to be P_{Si} (0.74 eV below CBM) and Al_{Si} (0.86 eV above VBM), respectively, for the substitutional impurities. With a clear charge-transfer mechanism of Al_{Si}, there have been experimental reports on the level position of Al_{Si} in SiO_2 to be 1.96 eV above the VBM.[8,15] Since this is an optical measurement, it does not include the relaxation effect of the final state, and therefore, one cannot compare directly with our calculated transition energy level, which should be thermally excited instead. To facilitate a direct comparison with the experiment, we have calculated the energy associated with the structural relaxation of Al_{Si} after it is charged to be 1.06 eV. We can then approximate the optical transition level (thermodynamic level+relaxation energy) to be 1.92 eV, which is in surprisingly good agreement with experiment. Similarly, for the P_{Si} case, it is approximated that the optical transition level (0.74 eV of thermodynamic level +3.05 eV of relaxation energy) to be 3.79 eV. While the experimental situation is more complicated in phosphate glass, the phosphorous-oxygen-hole center has been fitted to three absorption bands at 2.3, 2.89, and 3.82 eV.[12]

In general, n-type doping needs the CBM far away from the vacuum level whereas the p-type doping needs VBM close to the vacuum level.[43,44] Therefore, a complete success for both p-type and n-type doping is quite difficult for materials with wide band gap, such as ZnO and diamond.[45,46] It is, therefore, encouraging to see that SiO_2, a very wide band-gap material, possesses both relatively shallow donor and acceptor transition levels. Although we refer to these levels as "shallow," it is important to note that we mean relative to the very large gap of SiO_2. In an absolute sense, 0.8 eV is still quite deep in that it is very difficult to ionize at room temperature.

IV. CONCLUSION

Our systematic investigation of the doping properties of SiO_2 reveals no obvious doping asymmetry in the donor and acceptor level position, and only modest asymmetry in the impurity formation energy. With a GGA+U approach, we achieve a description of the local configuration of substituting impurities in SiO_2 which is quite consistent with EPR spectroscopy. It is found that SiO_2 can have both relatively shallow (with respect to the band gap) acceptor and donor

transition levels. Our predicted best candidates for *p*-type and *n*-type doping are Al_{Si} (0.86 eV above the VBM) and P_{Si} (0.74 eV below the CBM), respectively, both of which are consistent with previous experiments. These findings point out that this generally accepted insulator would have potential applications on forming an active layer for semiconductor devices. To utilize such new character for SiO_2, some critical problems must necessarily be solved, such as the migration of free carriers. Fortunately, the hopping-transfer mechanism of holes in disordered SiO_2 has been predicted.[47] Furthermore, the great success of the organic/polymer on electronic devices provides a good example for an insulating material being used as semiconductor. We expect some procedures,[48,49] such as codoping[50] or band-gap reduction,[51] would further lower the acceptor/donor levels to meet the ultimate acquirement of practical applications.

ACKNOWLEDGMENTS

We acknowledge the High Performance Computing Center (HPCC) of Jilin University and the Computational Center for Nanotechnology Innovations (CCNI) of Rensselaer Polytechnic Institute for supercomputer time. Works at JLU and RPI were supported by the National Science Foundation of China under Grant No. 90923037 and the U.S. Department of Energy under Grant No. DE-SC0002623. We gratefully thank W. Q. Tian, Q. D. Chen, Z. G. Chen, X. Meng, H. Yang, and H. Wang for their helpful discussions and technical support.

[1] *Defects in SiO_2 and Related Dielectrics: Science and Technology*, edited by G. Pacchioni, L. Skuja, and D. L. Griscom (Kluwer Academic, Dordrecht, 2000).
[2] K. C. Kao and G. A. Hockham, Proc. Inst. Electr. Eng. **113**, 1151 (1966).
[3] E. Gerstner, Nat. Phys. **5**, 780 (2009).
[4] R. Schnadt and J. Schneider, Phys. Kondens. Mater. **11**, 19 (1970).
[5] D. L. Griscom, G. H. Sigel, Jr., and R. J. Ginther, J. Appl. Phys. **47**, 960 (1976).
[6] R. H. D. Nuttall and J. A. Weil, Can. J. Phys. **59**, 1696 (1981).
[7] D. L. Griscom, E. J. Friebele, K. L. Long, and J. W. Fleming, J. Appl. Phys. **54**, 3743 (1983).
[8] B. K. Meyer, F. Lohse, J. M. Spaeth, and J. A. Weil, J. Phys. C: Solid State Phys. **17**, L31 (1984).
[9] B. Malo, J. Albert, F. Bilodeau, T. Kitagawa, D. C. Johnson, K. O. Hill, K. Hattori, Y. Hibino, and S. Gujrathi, Appl. Phys. Lett. **65**, 394 (1994).
[10] M. Magagnini, P. Giannozzi, and A. Dal Corso, Phys. Rev. B **61**, 2621 (2000).
[11] G. Pacchioni, F. Frigoli, D. Ricci, and J. A. Weil, Phys. Rev. B **63**, 054102 (2000).
[12] P. Ebeling, D. Ehrt, and M. Friedrich, Opt. Mater. **20**, 101 (2002).
[13] C. J. Walsby, N. S. Lees, R. F. C. Claridge, and J. A. Weil, Can. J. Phys. **81**, 583 (2003).
[14] D. Fischer, A. Curioni, S. Billeter, and W. Andreoni, Phys. Rev. Lett. **92**, 236405 (2004).
[15] J. To, A. A. Sokol, and S. A. French, J. Chem. Phys. **122**, 144704 (2005).
[16] C.-L. Kuo and G. S. Hwang, Phys. Rev. B **79**, 165201 (2009).
[17] G. Origlio, F. Messina, M. Cannas, R. Boscaino, S. Girard, A. Boukenter, and Y. Ouerdane, Phys. Rev. B **80**, 205208 (2009).
[18] R. A. Weeks, R. H. Magruder III, R. Galyon, and R. A. Weller, J. Non-Cryst. Solids **351**, 1727 (2005).
[19] H. Hosono, K. Kajihara, M. Hirano, and M. Oto, J. Appl. Phys. **91**, 4121 (2002).
[20] M. C. Paul, D. Bohra, A. Dhar, R. Sen, P. K. Bhatnagar, and K. Dasgupta, J. Non-Cryst. Solids **355**, 1496 (2009).
[21] M. Modreanu, N. Tomozeiu, P. Cosmin, and M. Gartner, Thin Solid Films **337**, 82 (1999).
[22] S. Koizumi, K. Watanabe, M. Hasegawa, and H. Kanda, Science **292**, 1899 (2001).
[23] J. Li and Z. Y. Fan, Appl. Phys. Lett. **89**, 213510 (2006).
[24] X. Zhang, X. M. Li, T. L. Chen, C. Y. Zhang, and W. D. Yu, Appl. Phys. Lett. **87**, 092101 (2005).
[25] P. Hohenberg and W. Kohn, Phys. Rev. **136**, B864 (1964).
[26] W. Kohn and L. J. Sham, Phys. Rev. **140**, A1133 (1965).
[27] G. Kresse and J. Furthmuller, Phys. Rev. B **54**, 11169 (1996).
[28] P. E. Blöchl, Phys. Rev. B **50**, 17953 (1994).
[29] J. P. Perdew and Y. Wang, Phys. Rev. B **33**, 8800 (1986).
[30] J. P. Perdew, K. Burke, and M. Ernzerhof, Phys. Rev. Lett. **77**, 3865 (1996).
[31] J. Lægsgaard and K. Stokbro, Phys. Rev. Lett. **86**, 2834 (2001).
[32] V. I. Anisimov, F. Aryasetiawan, and A. I. Lichtenstein, J. Phys.: Condens. Matter **9**, 767 (1997).
[33] M. Nolan and G. W. Watson, J. Chem. Phys. **125**, 144701 (2006).
[34] S. B. Zhang and J. E. Northrup, Phys. Rev. Lett. **67**, 2339 (1991).
[35] L. A. J. Garvie, P. Rez, J. R. Alvarez, and P. R. Buseck, Solid State Commun. **106**, 303 (1998).
[36] S. B. Zhang, J. Phys.: Condens. Matter **14**, R881 (2002).
[37] A. Janotti, S. B. Zhang, S.-H. Wei, and C. G. Van de Walle, Phys. Rev. Lett. **89**, 086403 (2002).
[38] M. Kohketsu, H. Kawazoe, and M. Yamane, J. Non-Cryst. Solids **105**, 69 (1988).
[39] Y. Uchida, J. Isoya, and J. A. Well, J. Phys. Chem. **83**, 3462 (1979).
[40] H. A. Jahn and E. Teller, Proc. R. Soc. London, Ser. A **161**, 220 (1937).
[41] *CRC Handbook of Chemistry and Physics*, edited by D. R. Lide (CRC Press, Boca Raton, Florida, 2004).
[42] *Properties of Crystalline Silicon*, edited by R. Hull (INSPEC, The Institution of Electrical Engineers, London, 1999).
[43] A. Zunger, Appl. Phys. Lett. **83**, 57 (2003).
[44] S. B. Zhang, S.-H. Wei, and A. Zunger, Phys. Rev. Lett. **84**, 1232 (2000).
[45] D. C. Look and B. Claflin, Phys. Status Solidi B **241**, 624 (2004).

[46] Z. Teukam, J. Chevallier, C. Saguy, R. Kalish, D. Ballutaud, M. Barbé, F. Jomard, A. Tromson-Carli, C. Cytermann, J. E. Butler, M. Bernard, C. Baron, and A. Deneuville, Nature Mater. **2**, 482 (2003).

[47] M. Farnesi Camellone, T. D. Kühne, and D. Passerone, Phys. Rev. B **80**, 033203 (2009).

[48] S. Limpijumnong, S. B. Zhang, S.-H. Wei, and C. H. Park, Phys. Rev. Lett. **92**, 155504 (2004).

[49] Y. Yan and S.-H. Wei, Phys. Status Solidi B **245**, 641 (2008).

[50] D. Segev and S.-H. Wei, Phys. Rev. Lett. **91**, 126406 (2003).

[51] Y. Yan, J. Li, S.-H. Wei, and M. M. Al-Jassim, Phys. Rev. Lett. **98**, 135506 (2007).